Linear Least-Squares Method for Unbiased Estimation of T_1 From SPGR Signals

Lin-Ching Chang,[1,2*] Cheng Guan Koay,[2] Peter J. Basser,[2] and Carlo Pierpaoli[2]

The longitudinal relaxation time, T_1, can be estimated from two or more spoiled gradient recalled echo images (SPGR) acquired with different flip angles and/or repetition times (TRs). The function relating signal intensity to flip angle and TR is nonlinear; however, a linear form proposed 30 years ago is currently widely used. Here we show that this linear method provides T_1 estimates that have similar precision but lower accuracy than those obtained with a nonlinear method. We also show that T_1 estimated by the linear method is biased due to improper accounting for noise in the fitting. This bias can be significant for clinical SPGR images; for example, T_1 estimated in brain tissue (800 ms < T_1 < 1600 ms) can be overestimated by 10% to 20%. We propose a weighting scheme that correctly accounts for the noise contribution in the fitting procedure. Monte Carlo simulations of SPGR experiments are used to evaluate the accuracy of the estimated T_1 from the widely-used linear, the proposed weighted-uncertainty linear, and the nonlinear methods. We show that the linear method with weighted uncertainties reduces the bias of the linear method, providing T_1 estimates comparable in precision and accuracy to those of the nonlinear method while reducing computation time significantly. Magn Reson Med 60:496–501, 2008. © 2008 Wiley-Liss, Inc.

Key words: T_1 estimation; linear model; accuracy; uncertainties; SPGR signals

Clinical imaging of the longitudinal relaxation time, T_1, in human subjects has several potential applications, including perfusion imaging (1), dynamic contrast imaging (2), assessment of Parkinson's disease (3), assessment of schizophrenia (4) and multiple sclerosis (5), and quantification of myocardial blood flow (6). In spite of its potential clinical utility, quantitative T_1 mapping is not routinely used due to the long scanning time inherent in inversion recovery sequences. Recently, however, the acquisition of high-resolution T_1 maps in a clinically feasible time frame has been demonstrated with Driven Equilibrium Single Pulse Observation of T_1 (DESPOT1) (7,8). DESPOT1 derives T_1 from two or more spoiled gradient recalled echo (SPGR) images acquired with a constant TR and different flip angles. The T_1 maps have been computed on a voxel-by-voxel basis using linear least squares (LLS) fitting of a linear transformation of the function relating signal intensity, flip angle, TR, T_1, and equilibrium longitudinal magnetization, M_0. This transformed LLS fitting method—first described by Gupta (9) in 1977, which we denote as Gupta's LLS (GLLS), and used in many previous works (7,8,10–12)—has the advantage of being computationally efficient. However, our preliminary study found that the estimated T_1 using GLLS was generally biased and overestimated (13).

In this work, we study systematically the bias in T_1 computed from SPGR signals when different fitting methods are used. Monte Carlo simulations provide a detailed evaluation of the accuracy of T_1 using GLLS and nonlinear least squares (NLS) methods in several experimental conditions. We also evaluate the performance of an intensity-based weighted LLS approach (ILLS) proposed by Deoni et al. (14). The ILLS method assigns greater weight to high signal-to-noise ratio (SNR) points in order to increase the precision of estimated T_1. Finally, we propose a new LLS approach that uses weighted uncertainties in the fitting (WLLS). The proposed WLLS method weights each image with the uncertainty that takes into account the adjustment of noise contribution due to the rearrangement of a nonlinear model into a linear one. Numerical and human brain data simulations are used to compare the accuracy of T_1 estimates using the GLLS, ILLS, WLLS, and NLS methods.

THEORY

NLS Method

The measured SPGR signal intensity, s_i, is a function of the longitudinal relaxation time, T_1; the repetition time (TR); the flip angle, α_i; and the equilibrium longitudinal magnetization, M_0:

$$s_i = \frac{M_0\left(1 - \exp\left(-\frac{TR}{T_1}\right)\right)\sin(\alpha_i)}{1 - \exp\left(-\frac{TR}{T_1}\right)\cos(\alpha_i)}. \quad [1]$$

The NLS approach estimates T_1 and M_0 from Eq. [1] by minimizing the following χ^2 objective function:

$$\chi^2_{NLS}(M_0, T_1) = \sum_{i=1}^{n} \frac{1}{\sigma_i^2}\left(s_i - M_0\sin(\alpha_i)\frac{1 - \exp\left(-\frac{TR}{T_1}\right)}{1 - \exp\left(-\frac{TR}{T_1}\right)\cos(\alpha_i)}\right)^2, \quad [2]$$

where σ_i is the expected signal standard deviation (SD) due to noise. When the SNR, s_i/σ_i, is greater than 5, σ_i can be considered as a constant in all images, i.e., $\sigma_1 = \sigma_2$

[1]Department of Electrical Engineering and Computer Science, Catholic University of America, Washington, DC, USA.

[2]National Institute of Child Health and Human Development, National Institutes of Health, Bethesda, Maryland, USA.

Grant sponsors: National Institute of Child Health and Human Development; National Institute on Drug Abuse; National Institute of Mental Health; National Institute of Neurological Disorders and Stroke; NIH Neuroscience Blueprint.

*Correspondence to: Lin-Ching Chang, Catholic University of America, 620 Michigan Ave. NE, Washington, DC 20064. E-mail: changl@cua.edu

Received 30 March 2007; revised 20 March 2008; accepted 24 March 2008.

DOI 10.1002/mrm.21669

Published online in Wiley InterScience (www.interscience.wiley.com).

$= \ldots = \sigma_n = \sigma$. But when s_i/σ_i is less than 5, this assumption becomes invalid (15).

LLS Method

In the LLS method, the linear equation is obtained by assuming that TR is a constant. By rearranging Eq. [1] and denoting $\exp(-TR/T_1)$ by E_1, we have:

$$\frac{s_i}{\sin(\alpha_i)} = E_1\frac{s_i}{\tan(\alpha_i)} + M_0(1 - E_1). \quad [3]$$

Equation [3] can be rewritten in a more explicit linear notation as $\boldsymbol{y} = b\boldsymbol{x} + a$ with $y_i = f(s_i) = s_i/\sin(\alpha_i)$, $x_i = g(s_i) = s_i/\tan(\alpha_i)$, $b = E_1$, and $a = M_0(1 - E_1)$.

The slope, b, and the y-intercept, a, can be estimated by linear regression (16,17), i.e., by minimizing the χ^2 objective function:

$$\chi^2_{LLS}(a,b) = \sum_{i=1}^{n} w(i)x(y_i - bx_i - a)^2$$

$$= \sum_{i=1}^{n} w(i)x\left(\frac{s_i}{\sin(\alpha_i)} - E_1\frac{s_i}{\tan(\alpha_i)} - M_0(1 - E_1)\right)^2. \quad [4]$$

The GLLS method proposed by Gupta (9) uses the linearization approach of Eq. [3] with $w_{GLLS}(i) = 1/\sigma_i^2$, which has been used in many previous works (7,8,10–12). Note that σ_i is the SD of the measurement error on y_i and is generally assumed to be a constant in a linear model when measurements of y_i are independent. The assumption in the widely-used GLLS method that the SD of y_i is the same for all data points (i.e., $\sigma_i = \sigma$) is incorrect because the experimental errors are distorted by the nonlinear to linear transformation. Under this assumption, T_1 and M_0 can then be calculated with the representation of a and b (10,16): $T_1 = -TR/\ln b$ and $M_0 = a/(1 - b)$.

An empirical weighting approach for the LLS fitting was introduced in Ref. 14. This method, which we call the ILLS method, assigns greater weight to data points with higher signal intensity in an attempt to increase the precision of estimated T_1, and solves Eq. [3] by minimizing Eq. [4] with a different weighting function defined in Ref. 14: $w_{ILLS}(i) = s_{\alpha_i}/s_{\alpha_E}$, where s_{α_i} is the signal intensity acquired with flip angle α_i, and S_{α_E} is the signal intensity acquired with the Ernst angle. T_1 and M_0 can be calculated as above.

Experimental errors are generally distorted when a nonlinear model is transformed to a linear one. A weighting function that accommodates the distorted uncertainties can be derived by using the error propagation theory (16) (see Appendix). Here, we can rewrite the χ^2 objective function for the NLS approach (Eq. [2]) as:

$$\chi^2_{NLS} = \sum_{i=1}^{n}\frac{1}{\sigma_i^2}\left(s_i - M_0\sin(\alpha_i)\frac{1 - E_1}{1 - E_1\cos(\alpha_i)}\right)^2$$

$$= \sum_{i=1}^{n}\frac{1}{\sigma_i^2}\left(\frac{\sin(\alpha_i)}{1 - E_1\cos(\alpha_i)}\right)^2\left(\frac{s_i}{\sin(\alpha_i)} - E_1\frac{S_i}{\tan(\alpha_i)} - M_0(1 - E_1)\right)^2. \quad [5]$$

Notice that Eq. [5] is similar in form to the objective function in LLS (i.e., Eq. [4]), and can be considered as a new weighted LLS method, which we denote as WLLS. By comparing Eq. [4] with Eq. [5], the weighting function of WLLS can therefore be defined as $w_{WLLS}(i) = \frac{1}{\sigma_i^2}\left(\frac{\sin(\alpha_i)}{1 - E_1\cos(\alpha_i)}\right)^2$.

Here, we have established the theoretical connection between the nonlinear and proposed weighted linear methods based on the approach used in Ref. 18. The proposed WLLS method is equivalent to the NLS method in principle because Eq. [5] is derived directly from Eq. [2], and no transformation or approximation is applied during the rearrangement.

We now want to minimize Eq. [5] with respect to a and b. However, the occurrence of b ($= E_1$) in the denominator of Eq. [5] makes the task of fitting considerably harder. An iterative least-squares fitting approach can be used here to find the optimal solution (19), and the GLLS method can be used as an initial solution. There are strategies for fitting a line in this situation (17,20,21), any of which can be applied here. We use Brent's method as described in Refs. 22 and 23, which is a reasonable strategy for minimizing a general one-dimensional function so that the minimization with respect to b is also minimized with respect to a.

MATERIALS AND METHODS

Numerical Simulations

We evaluated the accuracy and precision of different fitting algorithms in several experimental conditions by performing Monte Carlo simulations. Noise-free SPGR signals were generated using Eq. [1] given a fixed TR value, multiple flip angles, a single expected value of the equilibrium longitudinal magnetization M_0, and various expected values of T_1. Different SNR (SNR_0) levels were simulated by adding Gaussian noise (s_{noise}) in quadrature with zero mean and variable SD, σ, to the noise-free SPGR signals, i.e., $s_{spgr} = \sqrt{(s_{noise\text{-}free\text{-}spgr} + s_{noise^1})^2 + s_{noise^2}}$ (24). The noise level is defined as M_0 divided by the signal SD, i.e., $SNR_0 = M_0/\sigma$. We calculated T_1 by fitting the synthetic SPGR signals using the GLLS, WLLS, and NLS fitting approaches. The results reported in the next section are computed with TR = 10 ms, $M_0 = 3000$, and $T_1 = 600$, 800, 1000, 1200, 1600, or 2000 ms. The two optimal flip angles for the chosen T_1 were computed according to the formula in Refs. 10 and 14. For example, given $T_1 = 1000$ ms, TR = 10 ms, and $M_0 = 3000$, the optimal flip angles are 3.35° and 19.38°. Six SPGR images were used in simulations with repeated experiments of the two optimal angles without averaging. Noise levels were tested with SNR_0 ranging from 30 to 300. Each set of parameters was repeated 131,072 times.

Human Brain Simulation

A separate set of simulations was aimed at assessing the accuracy of estimated T_1 for experimental conditions compatible with clinical studies of the human brain at 1.5T. We collected a high-quality SPGR dataset of the brain of a healthy male volunteer. Images were acquired with a DESPOT1 sequence (7) in axial view with 0.9375-mm^2 in-plane resolution, 2-mm slice thickness, TR = 8 ms, and 20 different flip angles. The scan time was about 20 min (1 min per flip angle). This high-quality SPGR dataset was used to compute a T_1 and an M_0 map using the NLS method, and the values obtained in each voxel of the brain were assumed to be error-free. From these "gold standard" T_1 and M_0 maps, and a given set of TR and flip angles, we then generated synthetic noise-free SPGR images by computing the signal intensity in each voxel using Eq. [1]. Gaussian noise in quadrature with zero mean and a given SD, $\sigma = 100$, was added to the noise-free synthetic SPGR images as described in the previous paragraph. In the resultant SPGR brain images that have $SNR_0 = M_0/\sigma$ ranging from 90 to 150 throughout most areas of the brain tissue, we then computed the T_1 map by fitting these synthetic human brain data with GLLS, WLLS, and ILLS methods. This procedure was repeated 500 times and an averaged T_1 map was created by taking the mean value of T_1 from the 500 repeats on a voxel-by-voxel basis. The results reported in the next section are computed using TR = 10 ms and six SPGR images, with the flip angles in each image equal to 3°, 6°, 9°, 12°, 15°, and 18°, respectively.

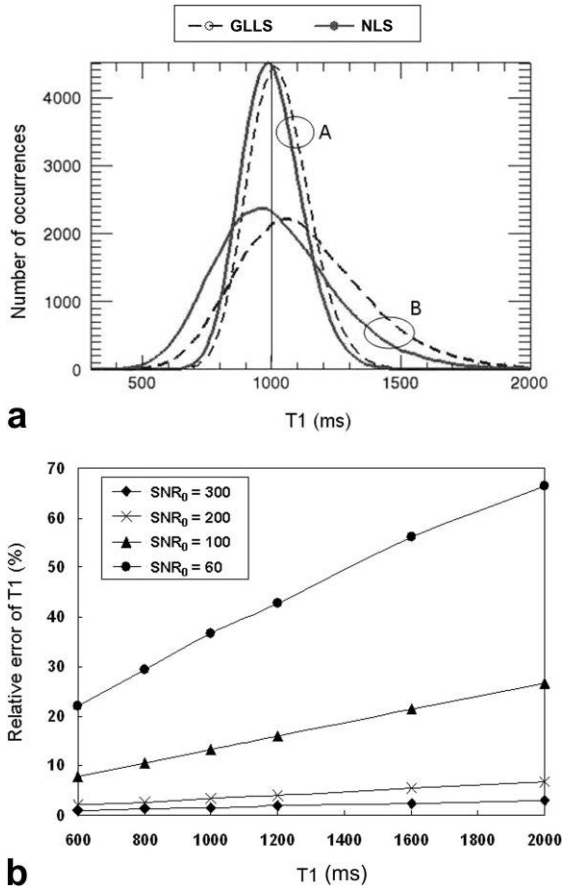

FIG. 1. (**a**) Distribution of T_1 using six SPGR images (three replicates of two flip angles) with two different noise levels (group A: M_0/σ = 200, group B: $M_0/\sigma = 100$). The true T_1 value is 1000 ms. (**b**) Relative errors of T_1 using the GLLS approach at different noise levels (SNR_0 = 60, 100, 200, and 300) with the true T_1 value set to 600, 800, 1000, 1200, 1600, and 2000 ms. Relative error of $T_1 = 100 \times$ (Estimated T_1 – True T_1)/True T_1.

RESULTS

Figure 1 demonstrates the behavior of T_1 bias when estimating T_1 from SPGR signals using the GLLS method. Figure 1a shows that the distributions of T_1 obtained with GLLS are biased, with the bias more pronounced at low SNR_0 since the distribution of T_1 is shifted more to the right when the M_0/σ ratio is lower (group B in Fig. 1a). The precision of estimated T_1 from GLLS and NLS is similar since the distributions under the same SNR_0 are similar. Figure 1b shows the bias as a function of T_1 and SNR_0. For a given SNR_0, the relative error of T_1 is found to be proportional to the value of T, although the accuracy of T_1 is relatively unaffected by the value of T_1 in a high SNR_0 regime (>200). When given the same T_1, the relative error of T_1 was found to be inversely proportional to SNR_0. The precision of estimated T_1 from GLLS and NLS is also similar (data not shown).

The results in Fig. 2 show that the WLLS virtually eliminates the T_1 bias for a broad range of SNR_0 and T_1 values. Figure 2a shows that WLLS and NLS produce comparable accuracy of T_1 at all SNR_0's tested, while GLLS overestimates T_1 progressively as SNR_0 decreases. Figure 2b shows that the bias of T_1 is corrected in WLLS with the relative error less than 5% regardless of the T_1 value. T_1's estimated using WLLS and NLS have similar precision; T_1 estimated using GLLS has slightly lower precision than T_1 estimated using NLS, in agreement with previous reports (10,12) (data not shown).

Figure 3 shows maps of the relative error on the estimated T_1 in the synthetic human brain data using the GLLS, ILLS, and WLLS methods. The results shown in Fig. 3 were scaled in the range of negative/positive 20% and the gray background corresponds to zero. The relative error of GLLS is consistently higher than that of WLLS in the brain tissue, and is positive, indicating that T_1 is overestimated. The error of ILLS is higher than the error of WLLS in most of the brain tissue. Although the error of ILLS is generally lower than that of GLLS, it shows a strong dependency on T_1, resulting in an undesirable tissue-dependent pattern. It is also notable that the bias in the cerebral spinal fluid (CSF) regions is higher than the bias in the brain parenchyma for all three methods, with GLLS and WLLS showing positive bias and ILLS negative bias.

DISCUSSION AND CONCLUSIONS

The linear model for T_1 estimation presented by Gupta (9) and used in many previous works (7–12) is an example of linearization. In general, weighted uncertainties must be used with linearly transformed data because the transformation distorts the experimental errors (16). However, Gupta's linear regression assumes that the scatter of points

around the line follows a Gaussian distribution and that the SD is the same at every data point. In this work we show that neglecting such adjustments to the uncertainty produces significant errors in the T_1 estimation. The magnitude of T_1 bias can be related to the true T_1 value, and the experiment design affecting SNR, such as the TR, flip angles, image resolution, and receiver coil. For clinical whole-brain SPGR data acquired at 1.5T with a single-channel receiver coil (TR = 8 ms, 1 mm^3 resolution, and flip angles = 2°, 3°, 14°, and 17°), the SNR_0 ranges from 100 to 200 in brain tissue; the T_1 value can be overestimated by 10–20%.

In many applications, achieving an unbiased estimation of the desired parameters from transformed data is achieved by computing weighted uncertainties with error analysis and error propagation techniques. We show such an approach in the Appendix. Moreover, we have derived a new WLLS model for T_1 estimation directly from the nonlinear model without using any transformation or approximation. This is an interesting result because converting a nonlinear model to a linear one using direct analytical derivation without approximations is not always possible.

It is worth emphasizing that the bias of the linear model depends not only on the measurement errors in the abscissa and the ordinate, but also on their covariance since the measurements in both axes are no longer independent. Our simulations show that using correct weights on the abscissa and the ordinate in Gupta's formula will not result in unbiased estimates of T_1; a covariance term must be included (see Appendix).

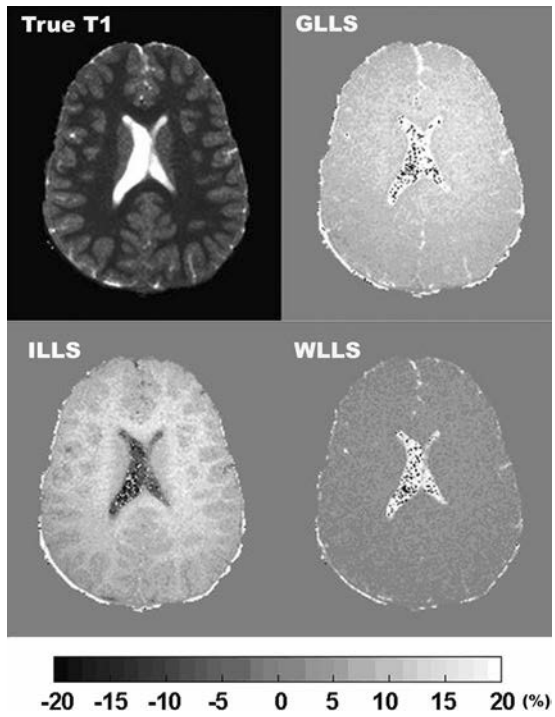

FIG. 3. Relative error of T_1 on a selected slice of synthetic human brain data using the GLLS, WLLS, and ILLS methods in the fitting procedure. The true T_1 map of the same slice is shown in the upper left panel for reference.

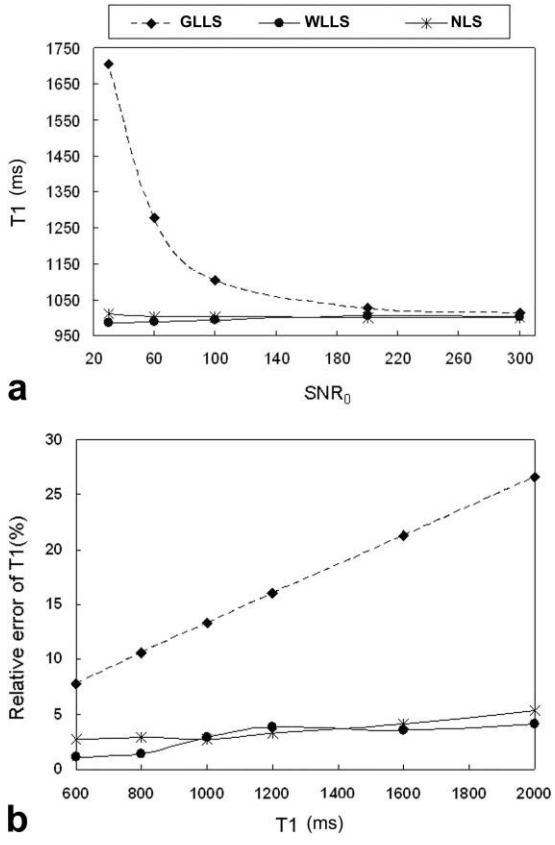

FIG. 2. (**a**) Estimated T_1 using GLLS, WLLC, and NLS methods assuming a true T_1 value of 1000 ms, and (**b**) relative error of T_1 using GLLS, WLLS, and NLS methods with SNR_0 = 100. Six SPGR images, consisting of three replicates of two flip angles without averaging, were used in both a and b.

The previously proposed intensity-based weighting approach, ILLS, improves the accuracy of the estimated T_1 in some brain areas. However, with this method the bias shows an undesirable strong dependence on the values of T_1. In general, all linear methods—GLLS, ILLS, and WLLS—are least accurate in estimating T_1 in regions with high T_1, such as CSF, but GLLS and WLLS overestimate while ILLS underestimates. This poor performance in CSF has little practical relevance because accuracy in CSF is generally biologically less important than in brain parenchyma. Moreover, the estimation of T_1 from SPGR data in regions of high T_1, such as CSF, is already problematic given that the SD of T_1 measured from SPGR signals is proportional to the square of T_1 (10). The SPGR simulations we performed in the human brain used experimental parameters aimed at optimizing typical values of T_1 in gray ($T_1 \sim 950$ ms) and white ($T_1 \sim 600$ ms) matter, but not in CSF ($T_1 \sim 4500$ ms), resulting in a magnification of potential problems in regions with high T_1. Although the results of the WLLS method may be affected by rectified noise, which is not accounted for in all models previously studied, signal correction methods such as those of Koay et al. (15) and Henkelman (24) may be used to resolve this problem. For scanning protocols used in clinical applications, the SNR in brain parenchyma is generally high enough to avoid effects from rectified noise.

T_1 bias can also originate from sources that are not addressed here. For example, flip angle variations caused by B_1 inhomogeneity can cause additional errors in T_1 estimation; approaches have been proposed to correct these inaccuracies (12,25). To get a robust estimation of T_1 from clinical SPGR signals, correcting B_1 inhomogeneity or the flip angles should be considered in addition to using the proposed weighted linear method in the fitting.

In terms of computation speed, WLLS is slower than GLLS since WLLS may need several iterations of linear regression while GLLS needs only one; however, WLLS is still computationally faster than NLS. For example, the numerical simulation (Fig. 2) we performed took 11–12 s for GLLS and 59–65 s for WLLS, but 17–29 min for NLS. The difference in time for the same method varied due to different noise levels.

WLLS and NLS are comparable in terms of both precision and accuracy in estimating T_1 and M_0. WLLS, however, was found to be more stable than NLS at low SNR_0 (i.e., a lower occurrence of T_1 outliers such as negative T_1 values). We suspect that this instability of the NLS approach is due to the known large-residuals problem in nonlinear regression (26). The Newton method for nonlinear fitting is known to be more robust for noisy data than the Levenberg-Marquardt based approaches (18). In future experiments we plan to systematically compare WLLS and NLS using the Newton method in testing the instability in the very low SNR regime. In general, clinical SPGR signals have higher SNR_0 and do not have the problem described above.

In this work we have shown that the relaxation time, T_1, estimated from the SPGR signals using the widely accepted LLS model is biased. The bias stems from neglecting to adjust uncertainties when transforming a nonlinear model into a linear one. We propose a weighting approach for the linear model that can be derived from the nonlinear model without any approximation. The proposed WLLS method yields estimated T_1 with precision and accuracy comparable to that obtained from nonlinear fitting while reducing the computation time significantly, enabling the generation of robust T_1 maps at the scanner console.

APPENDIX

Nonlinear regression is generally done without weighting or with constant weighting for all experimental data. For example, the σ_i values in Eq. [2] are the same for all SPGR data points. Giving equal weight to all data points is appropriate when the experimental uncertainty is expected to be the same in all measurements. When transforming a nonlinear function into a linear function, however, we must use weighted (or adjusted) uncertainties σ_i instead of σ_i to account for the transformation of the dependent variables (16). In general, if we fit the function $f(u)$ rather than u, the uncertainties in the measured quantities must be modified using the following formula (16):

$$\sigma_i = \sigma_{f(u_i)} = \frac{\partial f(u_i)}{\partial u_i}\sigma_i. \qquad [A1]$$

Note that the uncertainties should be modified in both abscissa and ordinate in the linear form of LLS (Eq. [3]) since both y_i and x_i are now subject to measurement errors on signals, s_i. Therefore, we have

$$\sigma_{y_i}^2 = \left(\frac{\partial f(s_i)}{\partial s_i}\right)^2 \sigma_i^2 = \left(\frac{1}{\sin(\alpha_i)}\right)^2 \sigma^2 \qquad [A2]$$

$$\sigma_{x_i}^2 = \left(\frac{\partial g(s_i)}{\partial s_i}\right)^2 \sigma_i^2 = \left(\frac{1}{\tan(\alpha_i)}\right)^2 \sigma^2. \qquad [A3]$$

Also note that the measurement errors due to noise in the abscissa and the ordinate are not independent; therefore, the covariance term between the measurement errors of y_i and x_i should also be taken into account:

$$\sigma_{x_i y_i}^2 = \frac{\partial f(s_i)}{\partial s_i} \times \frac{\partial g(s_i)}{\partial s_i} \times \sigma_i^2 = \left(\frac{1}{\sin(\alpha_i)}\right)\left(\frac{1}{\tan(\alpha_i)}\right)\sigma^2. \qquad [A4]$$

When applying the correct weighted uncertainties to Gupta's linear model—which we denote as WLLS—using the error propagation equation described in Refs. 16 and 25, we use the new variance that takes the uncertainties in both y_i and x_i, and their covariance term into account:

$$\begin{aligned} Var(\sigma_i) &= Var(y_i - bx_i - a) \\ &= \left(\frac{1}{\sin(\alpha_i)}\right)^2 \sigma_i^2 + b^2\left(\frac{1}{\tan(\alpha_i)}\right)^2 \sigma_i^2 \\ &\quad - 2b\left(\frac{1}{\sin(\alpha_i)}\right)\left(\frac{1}{\tan(\alpha_i)}\right)\sigma_i^2 \\ &= \left(\frac{1 - b\cos(\alpha_i)}{\sin(\alpha_i)}\right)^2 \sigma_i^2 \end{aligned} \qquad [A5]$$

The transformed linear equation therefore has the following χ^2 objective function (16,17,20):

$$\chi_{WLLS}^2(a,b) = \sum_{i=1}^{n} w(i)x(y_i - a - bx_i)^2, \qquad [A6]$$

where $w_{WLLS}(i) = \frac{1}{Var(\sigma_i)} = \frac{1}{\sigma_i^2}\left(\frac{\sin(\alpha_i)}{1 - b\cos(\alpha_i)}\right)^2$

Note that $\sigma_i = \sigma$ is a constant and therefore can be factored out.

ACKNOWLEDGMENTS

We thank the anonymous reviewers for their helpful comments, Dr. Sean Deoni for providing the DESPOT1 sequence used for data acquisition, and Ms. Liz Salak for editing the manuscript.

REFERENCES

1. Detre JA, Leigh JS, Williams DS, Koretsky AP. Perfusion imaging. Magn Reson Med 1992;23:37–45.
2. Gowland P, Mansfield P, Bullock P, Stehling M, Worthington B, Firth J. Dynamic studies of gadolinium uptake in brain tumors using inversion-recovery echo-planar imaging. Magn Reson Med 1992;26:241–258.

3. Vymazal J, Righini A, Brooks RA, Canesi M, Mariani C, Leonardi M, Pezzoli G. T1 and T2 in the brain of healthy subjects, patients with Parkinson disease, and patients with multiple system atrophy: relation to iron content. Radiology 1999;211:489–495.
4. Williamson P, Pelz D, Merskey H, Morrison S, Karlik S, Drost D, Carr T, Conlon P. Frontal, temporal, and striatal proton relaxation times in schizophrenic patients and normal comparison subjects. Am J Psychiatry 1992;149:549–551.
5. Larsson HB, Frederiksen J, Petersen J, Nordenbo A, Zeeberg I, Henriksen O, Olesen J. Assessment of demyelination, edema, and gliosis by in vivo determination of T1 and T2 in the brain of patients with acute attack of multiple sclerosis. Magn Reson Med 1989;11:337–348.
6. Zhang H, Shea SM, Park V, Li D, Woodard PK, Gropler RJ, Zheng J. Accurate myocardial T1 measurements: toward quantification of myocardial blood flow with arterial spin labeling. Magn Reson Med 2005; 53:1135–1142.
7. Deoni SC, Rutt BK, Peters TM. Rapid combined T1 and T2 mapping using gradient recalled acquisition in the steady state. Magn Reson Med 2003;49:515–526.
8. Deoni SC, Peters TM, Rutt BK. High-resolution T1 and T2 mapping of the brain in a clinically acceptable time with DESPOT1 and DESPOT2. Magn Reson Med 2005;53:237–241.
9. Gupta R. A new look at the method of variable nutation angle for the measurement of spin-lattice relaxation time using Fourier transform NMR. J Magn Reson 1977;25:231–235.
10. Wang HZ, Riederer SJ, Lee JN. Optimizing the precision in T1 relaxation estimation using limited flip angles. Magn Reson Med 1987;5: 399–416.
11. Fram EK, Herfkens RJ, Johnson GA, Glover GH, Karis JP, Shimakawa A, Perkins TG, Pelc NJ. Rapid calculation of T1 using variable flip angle gradient refocused imaging. Magn Reson Imaging 1987;5:201–208.
12. Cheng HL, Wright GA. Rapid high-resolution T1 mapping by variable flip angles: accurate and precise measurements in the presence of radiofrequency field inhomogeneity. Magn Reson Med 2006;55:566–574.
13. Chang LC, Koay CG, Deoni S, Pierpaoli C. Comparison of linear and non-linear fitting methods for estimating T1 from SPGR signals. In: Proceedings of the 15th Annual Meeting of ISMRM, Berlin, Germany, 2007 (Abstract 1775).
14. Deoni SC, Peters TM, Rutt BK. Determination of optimal angles for variable nutation proton magnetic spin-lattice, T1, and spin-spin, T2, relaxation times measurement. Magn Reson Med 2004;51:194–199.
15. Koay CG, Basser PJ. Analytically exact correction scheme for signal extraction from noisy magnitude MR signals. J Magn Reson 2006;179: 317–322.
16. Bevington P. Data reduction and error analysis for the physical sciences. New York: McGraw-Hill Book Company; 1969.
17. Press WH, Teukolsky SA, Vetterling WT, Flannery BP. Numerical recipes in C. Cambridge, UK: Cambridge University Press; 1992. p 666–670.
18. Koay CG, Chang LC, Carew JD, Pierpaoli C, Basser PJ. A unifying theoretical and algorithmic framework for least squares methods of estimation in diffusion tensor imaging. J Magn Reson 2006;182:115–125.
19. Chang LC, Jones DK, Pierpaoli C. RESTORE: robust estimation of tensors by outlier rejection. Magn Reson Med 2005;53:1088–1095.
20. Barker DR, Diana LM. Simple method for fitting data when both variables have uncertainties. Am J Phys 1974;42:224–227.
21. Reed BC. Linear least-squares fits with errors in both coordinates. Am J Phys 1989;57:642–646.
22. Brent R. Algorithms for minimization without derivatives. Englewood Cliffs, NJ: Prentice-Hall; 1973.
23. Press WH, Teukolsky SA, Vetterling WT, Flannery BP. Numerical recipes in C. Cambridge, UK: Cambridge University Press; 1992. p 402–405.
24. Henkelman RM. Measurement of signal intensities in the presence of noise in MR images. Med Phys 1985;12:232–233.
25. Deichmann R, Haase A. Quantification of T1 values by Snapshot-FLASH NMR imaging. J Magn Reson 1992;96:608–612.
26. Jorge N, Wright SJ. Numerical optimization. New York: Springer-Verlag, Inc.; 1999.